Inorg. Chem. **2003**, *42*, 1576–1583

dlf Complexes with Uniform Coordination Geometry: Structural and Magnetic Properties of an LnNi2 Core Supported by a Heptadentate Amine Phenol Ligand

Simon R. Bayly, Zhiquiang Xu, Brian O. Patrick, Steven J. Rettig, Maren Pink,[†] Robert C. Thompson,* and Chris Orvig*

Department of Chemistry, University of British Columbia, 2036 Main Mall, Vancouver, BC V6T 1Z1, Canada

Received August 30, 2002

The synthesis and physical characterization of a series of lanthanide (Ln^{III}) and nickel (Ni^{II}) mixed trimetallic complexes with the heptadentate (N_4O_3) amine phenol ligand H_3trn [tris(2′-hydroxybenzylaminoethyl)amine] has been accomplished in order to extend our understanding of how amine phenol ligands can be used to coaggregate *d*- and *f*-block metal ions and to investigate further the magnetic interaction between these ions. The one-pot reaction in methanol of stoichiometric amounts of H_3trn with $NiX_2 \cdot 6H_2O$ ($X = ClO_4$, NO_3) followed by addition of the corresponding $LnX_3 \cdot 6H_2O$ salt, and then base, produces complexes of the general formula $[LnNi_2(trn)_2]X \cdot nH_2O$. The complexes were characterized by a variety of analytical techniques. Crystals of five of the complexes were grown from methanol solutions and their structures were determined by X-ray analysis: $[PrNi_2(trn)_2(CH_3OH)]ClO_4 \cdot 4CH_3OH \cdot H_2O$, $[SmNi_2(trn)_2(CH_3OH)]NO_3 \cdot 4CH_3OH \cdot 2H_2O$, $[TbNi_2(trn)_2(CH_3OH)]NO_3 \cdot 4CH_3OH \cdot 3H_2O$, $[ErNi_2(trn)_2(CH_3OH)]NO_3 \cdot 6CH_3OH$, and $[LuNi_2(trn)_2(CH_3OH)]NO_3 \cdot 4.5CH_3OH \cdot 1.5H_2O$. The $[LnNi_2(trn)_2(CH_3OH)]^+$ complex cation consists of two octahedral Ni^{II} ions, each of which is encapsulated by the ligand trn^{3-} in an N_4O_2 coordination sphere with one phenolate O atom not bound to Ni^{II}. Each $[Ni(trn)]^-$ unit acts as a tridentate ligand toward the Ln^{III} ion via two bridging and one nonbridging phenolate donors. Remarkably, in all of the structurally characterized complexes, Ln^{III} is seven-coordinate and has a flattened pentagonal bipyramidal geometry. Such uniform coordination behavior along the whole lanthanide series is rare and can perhaps be attributed to a mismatch between the geometric requirements of the bridging and nonbridging phenolate donors. Magnetic studies indicate that ferromagnetic exchange occurs in the Ni^{II}/Ln^{II} complexes where Ln = Gd, Tb, Dy, Ho, or Er.

Introduction

Lanthanide and lanthanum compounds have attracted a great deal of interest in recent years because they have applications in medicinal inorganic chemistry and in materials science. In medicine, lanthanide complexes are exploited as contrast agents for magnetic resonance imaging (MRI)[1,2] and are developing in importance in other diagnostic procedures[3] and as radiotherapeutic drugs.[4] In materials science the most powerful permanent magnets known are transition metal−rare earth intermetallics.[5−7] However, in the search for molecular magnets, transition metal−rare earth species have rarely been investigated, and hence the nature of the magnetic interaction between Ln^{III} and transition metal ions is poorly understood. A reason for this is perhaps the difficulty in designing ligands that can effect the simultaneous coordination of *d*- and *f*-block metals to form discrete complexes or well-defined polymeric networks. Another

* To whom correspondence should be addressed. E-mail: orvig@chem.ubc.ca.

[†] X-ray Crystallographic Laboratory, University of Minnesota, Minneapolis, MN 55455. Present address: Indiana University Molecular Structure Center, Chemistry, Indiana University, 800 E. Kirkwood Ave., Bloomington, IN 47405.

(1) Lauffer, R. B. *Chem. Rev.* **1987**, *87*, 901.
(2) Caravan, P.; Ellison, J. J.; McMurry, T. J.; Lauffer, R. B. *Chem. Rev.* **1999**, *99*, 2293.
(3) Thunus, L.; Lejeune, R. *Coord. Chem. Rev.* **1999**, *184*, 125.
(4) Cutler, C. S.; Smith, C. J.; Ehrhardt, G. J.; Tyler, T. T.; Jurisson, S. S.; Deutsch, E. *Cancer Biother. Radiopharm.* **2000**, *15*, 531.
(5) Rauluszkiewicz, J.; Szymczak, H.; Lachowicz, H. K. *Physics of Magnetic Materials*; World Scientific: Singapore, 1985.
(6) Coey, J. M. D. *Endeavour* **1995**, *19*, 146.
(7) Müller, K. H.; Krabbes, G.; Fink, J.; Gruss, S.; Kirchner, A.; Fuchs, G.; Schultz, L. *J. Magn. Magn. Mater.* **2001**, *226*, 1370.

10.1021/ic0205278 CCC: $25.00
Published on Web 02/07/2003

significant challenge is the interpretation of magnetic data from ions with unquenched orbital angular momentum; to date most magnetic studies have been limited to those in which the lanthanide ion is Gd^{III}. With the advent of an empirical approach by Costes et al.[8] (also applied by Kahn et al.)[9] and theoretical models from Lloret and co-workers[10] and Sutter et al.,[11] the whole range of Ln^{III} ions is now being investigated. Except in our own laboratory (vide infra), the magnetic properties of mixed Ni^{II}/Ln^{III} complexes have received scant attention (one molecular NiGd example has been examined,[12] as has one set of Ni_3Gd_2 polymeric complexes[13]) and have only recently become of interest.[14−16]

For some time we have been exploring the chemistry of Ln^{III} ions with mixed-donor multidentate ligands, such as Schiff bases, amine phosphinates, amine pyridyl carboxylates, and in particular amine phenolates.[17−19] Recently, we have extended the scope of this research to the construction of oligometallic lanthanide complexes[20] and mixed lanthanide/transition metal ion arrays.[21] In this latter work the coaggregation of nickel (Ni^{II}) and lanthanide (Ln^{III}) metal ions in the presence of a tripodal amine phenol ligand, H_3-tam [1,1,1-tris(((2′-hydroxybenzyl)amino)methyl)ethane], provided a series of $LnNi_2$ trinuclear complexes that were characterized in terms of their crystal structures and magnetic properties. The magnetic data collected for a limited selection of these trinuclear complexes were interpreted as indicating that an antiferromagnetic exchange interaction occurred between the Ni^{II} and Ln^{III} ions and that this interaction decreased with the decreasing ionic radius of Ln^{III}.[21]

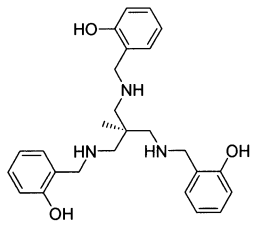

H_3tam

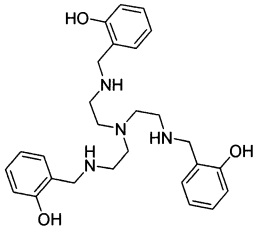

H_3trn

In the present study we have utilized the heptadentate amine phenol ligand H_3trn [tris(2′-hydroxybenzylamino-ethyl)amine][22] to investigate further the coaggregation of Ni^{II} and Ln^{III} ions with the subsequent aim of understanding the mechanism of the magnetic exchange interaction between the two metals. H_3trn possesses all the beneficial features inherent to amine phenol ligands: namely, it is hydrolytically stable, more geometrically flexible than its Schiff base analogue, and able to incorporate both lanthanide ions, with its hard (phenolato) donors, and transition metal ions, with these and its softer (amine) donors.

Experimental Section

Safety Note. *Although we have experienced no problems, perchlorate salts are potentially explosive. They should be handled with extreme care and used only in small quantities without heat.*[23,24]

Materials. Hydrated Ln^{III} perchlorates were obtained from Alfa either as the solid or as 50% (w/w) solutions in water, which were evaporated to dryness. Triethylamine was purchased from Fisher and was used as received. $Ni(ClO_4)_2·6H_2O$ was prepared from the corresponding carbonate by dissolution in perchloric acid. H_3trn was prepared according to our literature procedure.[22] Other commercially available solvents and chemicals were used without further purification.

Physical Measurements. Mass spectra were obtained on a Kratos Concept II H32Q (Cs^+, LSIMS) instrument in the positive ion detection mode, with a thioglycerol matrix. Infrared spectra were recorded as Nujol mulls (KBr windows) in the range 4000−400 cm^{-1} on a Mattson Galaxy Series FTIR-5000 spectrophotometer and were referenced to polystyrene (1601 cm^{-1}). Analyses of C, H, and N were performed by Mr. Peter Borda at the University of British Columbia. Variable-temperature magnetic susceptibility measurements were performed on a Quantum Design (MPMS) SQUID magnetometer on air-dried finely powdered samples (300−2 K, 500 G). A specially designed sample holder, as described previously,[25] was used to minimize the background signal. Magnetic susceptibilities were corrected for background. A diamagnetic correction was also applied (6.24×10^{-4} cm^3 mol^{-1}, plus 3.89×10^{-5} cm^3 mol^{-1} per water of crystallization).

(a) General Procedure for $[LnNi_2(trn)_2(H_2O)]NO_3·nH_2O$ (1−13) (all Ln except Ce and Pm). To a solution of $Ni(NO_3)_2·6H_2O$ (144 mg, 0.50 mmol) in methanol (5 mL) was added H_3trn (232 mg, 0.50 mmol) in methanol (10 mL). The pale blue solution was left to stir at room temperature (10 min), and hydrated $Ln(NO_3)_3$ was added (0.25 mmol). Upon addition of triethylamine (152 mg, 1.50 mmol) the solution became pale purple (for all Ln studied except Eu, which gave a pale green solution) and on standing (30 min) became cloudy. The solution was clarified by filtration and allowed to stand at room temperature. Purple (except Eu, which gave turquoise) crystals were formed overnight; these are stable in the parent solvent and lose coordinated (via MeOH−H_2O exchange) or lattice MeOH in air. Yields of the air-dried products varied widely (in the range 10−70%). A complete list of compounds prepared with their numbering and analytical data is presented in Table 1.

(8) Costes, J.-P.; Dahan, F.; Dupuis, A.; Laurent, J.-P. *Chem. Eur. J.* **1998**, *9*, 1617.
(9) Kahn, M. L.; Mathonière, C.; Kahn, O. *Inorg. Chem.* **1999**, *38*, 3697.
(10) Sanz, J. L.; Ruiz, R.; Gleizes, A.; Lloret, F.; Faus, J.; Julve, M.; Borrás-Almenar, J. J.; Journaux, Y. *Inorg. Chem.* **1996**, *35*, 7384.
(11) Sutter, J.-P.; Kahn, M. L.; Mortl, K. P.; Ballou, R.; Porcher, P. *Polyhedron* **2001**, *20*, 1593.
(12) Costes, J.-P.; Dahan, F.; Dupuis, A.; Laurent, J.-P. *Inorg. Chem.* **1997**, *36*, 4284.
(13) Kahn, M. L.; Lecante, P.; Verelst, M.; Mathoniere, C.; Kahn, O. *Chem. Mater.* **2000**, *12*, 3073.
(14) Lisowski, J.; Starynowicz, P. *Inorg. Chem.* **1999**, *38*, 1351.
(15) Knoeppel, D. W.; Liu, J. P.; Meyers, E. A.; Shore, S. G. *Inorg. Chem.* **1998**, *39*, 4828.
(16) Brechin, E. K.; Harris, S. G.; Parsons, S. G.; Winpenny, R. E. P. *J. Chem. Soc., Dalton Trans.* **1997**, 1665.
(17) Caravan, P.; Lowe, M. P.; Read, P. W.; Rettig, S. J.; Yang, L.-W.; Orvig, C. *J. Alloys Compd.* **1997**, *249*, 49.
(18) Caravan, P.; Mehrkhodavandi, P.; Orvig, C. *Inorg. Chem.* **1997**, *36*, 1316.
(19) Lowe, M. P.; Caravan, P.; Rettig, S. J.; Orvig, C. *Inorg. Chem.* **1998**, *37*, 1637.
(20) Setyawati, I. A.; Liu, S.; Rettig, S. J.; Orvig, C. *Inorg. Chem.* **2000**, *39*, 496.
(21) Xu, Z.; Read, P. W.; Hibbs, D. E.; Hursthouse, M. B.; Abdul Malik, K. M.; Patrick, B. O.; Rettig, S. J.; Seid, M.; Summers, D. A.; Pink, M.; Thompson, R. C.; Orvig, C. *Inorg. Chem.* **2000**, *39*, 508.
(22) Liu, S.; Gelmini, L. R.; Rettig, S. J.; Thompson, R. C.; Orvig, C. *J. Am. Chem. Soc.* **1992**, *114*, 6081.
(23) Wolsey, W. C. *J. Chem. Educ.* **1973**, *50*, A335.
(24) Cartwright, R. V. *Chem. Eng. News* **1983**, *61*, 4.
(25) Ehlert, M. K.; Rettig, S. J.; Storr, A.; Thompson, R. C.; Trotter, J. *Can. J. Chem* **1991**, *69*, 432.

Table 1. $[LnNi_2(trn)_2]NO_3$ (or ClO_4)·xH_2O Complexes Prepared in This Study (**1**−**21**) and Their Analytical Data

	% C		% H		% N		
complex	found	calcd	found	calcd	found	calcd	m/z of $[LnNi_2(trn)_2]^+$ [a]
$[LaNi_2(trn)_2]NO_3·5.5H_2O$ (**1**)	48.46	48.38	5.67	5.79	9.26	9.40	1177
$[PrNi_2(trn)_2]NO_3·6H_2O$ (**2**)	47.73	47.99	5.51	5.82	9.17	9.33	1179
$[NdNi_2(trn)_2]NO_3·2H_2O$ (**3**)	50.58	50.56	5.59	5.50	9.76	9.83	1184
$[SmNi_2(trn)_2]NO_3·2H_2O$ (**4**)	50.53	50.32	5.53	5.47	9.67	9.78	1192
$[EuNi_2(trn)_2]NO_3·4.5H_2O$ (**5**)	48.54	48.56	5.45	5.66	9.29	9.44	1191
$[GdNi_2(trn)_2]NO_3·6H_2O$ (**6**)	47.49	47.41	5.72	5.75	9.21	9.22	1198
$[TbNi_2(trn)_2]NO_3·5H_2O$ (**7**)	48.24	47.99	5.82	5.67	9.38	9.33	1197
$[DyNi_2(trn)_2]NO_3·3H_2O$ (**8**)	49.41	49.17	5.56	5.50	9.44	9.56	1202
$[HoNi_2(trn)_2]NO_3·5H_2O$ (**9**)	47.93	47.78	5.81	5.64	9.26	9.29	1203
$[ErNi_2(trn)_2]NO_3·5H_2O$ (**10**)	47.85	47.69	5.93	5.63	9.20	9.27	1206
$[TmNi_2(trn)_2]NO_3·4H_2O$ (**11**)	48.27	48.27	5.71	5.55	9.36	9.38	1207
$[YbNi_2(trn)_2]NO_3·4.5H_2O$ (**12**)	47.73	47.81	5.33	5.57	9.11	9.29	1212
$[LuNi_2(trn)_2]NO_3·4H_2O$ (**13**)	48.30	48.06	5.57	5.53	9.24	9.34	1213
$[LaNi_2(trn)_2]ClO_4·4H_2O$ (**14**)	48.07	48.06	5.71	5.53	8.05	8.31	1177
$[PrNi_2(trn)_2]ClO_4·3H_2O$ (**15**)	48.67	48.64	5.53	5.45	8.42	8.41	1179
$[NdNi_2(trn)_2]ClO_4·5H_2O$ (**16**)	47.52	47.32	5.53	5.59	7.99	8.18	1184
$[SmNi_2(trn)_2]ClO_4·6.5H_2O$ (**17**)	45.91	46.08	5.13	5.66	7.74	7.96	1192
$[GdNi_2(trn)_2]ClO_4·4H_2O$ (**18**)	47.24	47.37	5.41	5.45	7.96	8.18	1198
$[DyNi_2(trn)_2]ClO_4·5H_2O$ (**19**)	46.40	46.58	5.21	5.12	8.05	8.05	1202
$[HoNi_2(trn)_2]ClO_4·4H_2O$ (**20**)	47.08	47.15	5.46	5.43	8.11	8.15	1203
$[ErNi_2(trn)_2]ClO_4·3H_2O$ (**21**)	48.24	48.38	5.42	5.27	8.24	8.36	1206

[a] Found and calculated values for m/z of $[LnNi_2(trn)_2]^+$ were the same in each case.

Table 2. Crystallographic Data for Compounds **4a**, **7a**, **10a**, **13a**, and **15a**

	4a	**7a**	**10a**	**13a**	**15a**
formula	$C_{59}H_{90}N_9Ni_2O_{16}Sm$	$C_{59}H_{92}N_9Ni_2O_{17}Tb$	$C_{61}H_{94}N_9Ni_2O_{16}Er$	$C_{59.5}H_{91}N_9Ni_2O_{16}Lu$	$C_{59}H_{88}ClN_8Ni_2O_{16}Pr$
FW	1449.17	1475.75	1494.13	1480.80	1459.15
space group	$P\bar{1}$ (#2)	$P\bar{1}$ (#2)	$P\bar{1}$ (#2)	$P\bar{1}$ (#2)	$C2/c$ (#15)
a, Å	13.048(2)	13.0201(4)	13.104(1)	13.1652(1)	31.892(3)
b, Å	14.146(2)	14.1450(6)	14.300(2)	14.3387(1)	16.3008(7)
c, Å	19.710(3)	19.658(2)	19.611(1)	19.7309(2)	30.660(3)
α, deg	74.581(2)	74.430(2)	75.027(5)	74.813(1)	90.0
β, deg	83.723(2)	83.843(2)	83.182(3)	83.118(1)	122.064(2)
γ, deg	66.377(2)	66.666(2)	64.924(1)	65.074(1)	90.0
V, Å^3	3213.1(7)	3202.4(2)	3215.3(5)	3259.55(5)	13507.7(18)
Z	2	2	2	2	8
ρ_{obsd}, g cm^{-3}	1.498	1.530	1.543	1.509	1.435
T, K	193(2)	173(1)	173(1)	193(2)	180(1)
λ, Å	0.7107	0.7107	0.7107	0.7107	0.7107
μ, mm^{-1}	1.554	1.747	1.947	2.146	1.368
$R1$	0.0292	0.054	0.042	0.0249	0.055
w$R2a$	0.0751	0.121	0.0104	0.0630	0.052

[a] $R1$ and w$R2$ as defined in SHELX-93.

Table 3. Selected Bond Lengths (Å), Interatomic Distances (Å) and Angles (°) for **4a**, **7a**, **10a**, **13a** and **15a**

complex	**4a**	**7a**	**10a**	**13a**	**15a**
Ln−O1	2.464(2)	2.436(4)	2.418(3)	2.409(2)	2.509(5)
Ln−O2	2.408(2)	2.367(4)	2.328(3)	2.326(2)	2.458(4)
Ln−O3	2.237(2)	2.193(4)	2.168(3)	2.155(2)	2.285(4)
Ln−O4	2.411(2)	2.373(4)	2.342(3)	2.335(2)	2.476(5)
Ln−O5	2.444(2)	2.406(4)	2.382(3)	2.372(2)	2.492(5)
Ln−O6	2.207(2)	2.176(4)	2.150(3)	2.132(2)	2.260(3)
Ln−O7	2.519(3)	2.470(6)	2.438(4)	2.419(2)	2.541(5)
Ni1−O1	2.095(2)	2.091(4)	2.094(3)	2.108(2)	2.095(4)
Ni1−O2	2.018(2)	2.027(4)	2.027(3)	2.037(2)	2.046(5)
Ni1−N1	2.091(3)	2.092(6)	2.098(4)	2.111(3)	2.109(5)
Ni1−N2	2.095(2)	2.101(7)	2.098(4)	2.106(3)	2.089(5)
Ni1−N3	2.190(6)	2.235(6)	2.187(4)	2.201(3)	2.192(5)
Ni1−N7	2.099(3)	2.101(6)	2.108(4)	2.123(3)	2.108(7)
Ni2−O4	2.036(2)	2.042(4)	2.039(3)	2.051(2)	2.045(5)
Ni2−O5	2.086(2)	2.092(4)	2.084(4)	2.096(3)	2.070(5)
Ni2−N4	2.077(3)	2.073(7)	2.086(4)	2.094(3)	2.091(6)
Ni2−N5	2.105(3)	2.111(6)	2.110(4)	2.126(3)	2.114(5)
Ni2−N6	2.191(3)	2.188(6)	2.195(4)	2.202(3)	2.169(5)
Ni2−N8	2.110(3)	2.115(6)	2.121(4)	2.134(3)	2.111(6)
Ln−Ni1	3.5663(7)	3.5462(9)	3.5228(7)	3.5303(4)	3.6173(11)
Ln−Ni2	3.5804(7)	3.5601(9)	3.5433(7)	3.5498(4)	3.6285(12)
O1−Ln−O2	66.59(7)	66.98(14)	67.52(10)	67.78(7)	65.97(15)
O4−Ln−O5	66.04(8)	66.53(14)	66.61(12)	66.88(7)	65.17(14)
O1−Ni1−O2	81.11(9)	80.12(16)	79.61(11)	79.15(8)	81.32(17)
O4−Ni2−O5	79.87(9)	78.71(16)	77.98(12)	77.44(8)	81.11(18)

[a] Bond lengths and interatomic distances are given in angstroms; angles are given in degrees.

(b) General Procedure for $[LnNi_2(trn)_2]ClO_4·nH_2O$ (14−21). This was carried out with perchlorate salts in the place of nitrate salts in the above procedure, with the exception that after the addition of triethylamine to the solution, and prior to filtration, deionized water (2 mL) was added. Purple crystals were obtained directly from the solution for all Ln studied. The air-dried products were obtained in yields of 70−85% and are listed in Table 1.

X-ray Crystallographic Data Collection and Refinement of the Structures. Selected crystallographic data for complexes **4a**, **7a**, **10a**, **13a**, and **15a** are presented in Table 2 and selected bond lengths, interatomic distances and angles are shown in Table 3. The suffix **a** is used to distinguish these methanol-containing compounds from their hydrated air-dried counterparts in Table 1. An ORTEP drawing of the complex cation **13a** is presented in Figure 1. CIF files for **4a**, **7a**, **10a**, **13a**, and **15a** are included as Supporting Information.

$[SmNi_2(trn)_2(CH_3OH)]NO_3·4CH_3OH·2H_2O$ (4a) and $[LuNi_2(trn)_2(CH_3OH)]NO_3·4.5CH_3OH·1.5H_2O$ (13a). Data collection for **4a** (**13a**) was undertaken at the University of Minnesota. A violet crystal of approximate dimensions 0.3 × 0.3 × 0.2 (0.5 × 0.3 × 0.08) mm^3 was mounted on a glass capillary. Data collection was carried out on a Siemens SMART system with Mo Kα radiation (graphite monochromator) and a detector distance of 4.9 (4.9) cm. A randomly oriented region of reciprocal space was surveyed to the extent of 0.95 (1.3) spheres and to a resolution of 0.84 Å. Three major sections of frames were collected with 0.30° steps in ω at 4 (3) different ϕ settings and a detector position of −25° (−28°) in 2θ with a frame time of 15 (10) s.

The structure **4a** (**13a**) was solved and refined by use of SHELX-86[26] and SHELX-97.[27] A direct-methods solution was calculated

(26) Sheldrick, G. M. *SHELX-86*: University of Gottingen, Germany, 1985.
(27) Sheldrick, G. M. *SHELX97*: University of Gottingen, Germany, 1997.

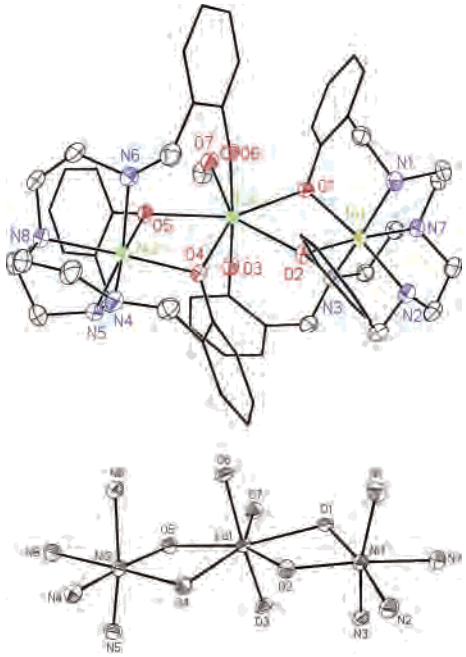

Figure 1. Structure of the $[LuNi_2(trn)_2(CH_3OH]^+$ cation in **13a** and expanded view of the Lu coordination sphere. Hydrogen atoms are omitted for clarity. Thermal ellipsoids are drawn at 50% probability and are omitted for ring carbon atoms.

that provided most non-hydrogen atoms from the E-map. Full-matrix least-squares/difference Fourier cycles were performed that located the remaining non-hydrogen atoms. All non-hydrogen atoms were refined with anisotropic displacement parameters. All hydrogen atoms were placed in ideal positions or found from the E-map and refined freely or as riding atoms with individual or group isotropic displacement parameters.

The structure of **4a** was found to contain the $[SmNi_2(trn)_2(CH_3OH)]^+$ complex cation, a nitrate anion, four methanol molecules, and two water molecules in the asymmetric unit. The methyl group of the coordinated solvent methanol is disordered. Both the nitrate and one methanol molecule (O14, C59) have rather large displacement parameters, which are due to disorder. However, the major site was refined as being 100% occupied since there are many minor sites that sum up to at most 4%.

Similarly, the asymmetric unit in the structure of **13a** contains the complex cation $[LuNi_2(trn)_2(CH_3OH)]^+$, four methanol molecules, one water molecule, and one molecule that is part of the time methanol and part of the time water. The methyl group of the methanol molecule coordinated to Lu is disordered. The counterion is disordered over two sites including the previously mentioned solvents (major site 51%). The void space created by the packing of the complex cation is completely filled by solvent.

$[TbNi_2(trn)_2(CH_3OH)]NO_3\cdot4CH_3OH\cdot3H_2O$ (7a), $[ErNi_2(trn)_2(CH_3OH)]NO_3\cdot6CH_3OH$ (10a), and $[PrNi_2(trn)_2(CH_3OH)]ClO_4\cdot4CH_3OH\cdot H_2O$ (15a). Data collection for **7a** (**10a**) (**15a**) was undertaken at the University of British Columbia. A purple crystal of approximate dimensions 0.20 × 0.15 × 0.05 (0.30 × 0.30 × 0.20) (0.30 × 0.25 × 0.15) mm^3 was mounted on a glass fiber. All measurements were made on a Rigaku/ADSC CCD area detector with graphite monochromated Mo Kα radiation. The data were collected to a maximum 2θ value of 55.9° (55.8°) (61.1°), by use of 0.50° (0.50°) (0.30°) oscillations with 51.0 (51.0) (20.0) s exposures. Sweeps of data were done with ϕ oscillations from 0.0° to 190.0° at $\chi = -90°$ and ω oscillations between −18.0° and 23.0° at $\chi = -90°$. The crystal-to-detector distance was 39.7 (39.8) (38.9) mm. The detector swing angle was −5.6° (5.6°) (−10.0°). The structures were solved by direct methods[28] and expanded by Fourier techniques.[29]

The material **7a** crystallizes with approximately four molecules of MeOH and three molecules of H_2O in the asymmetric unit. Due to large thermal motion, some of these molecules were refined isotropically, and in the case of the water molecules no hydrogens were found or included. All other non-hydrogen atoms were refined anisotropically.

The material **10a** crystallizes with approximately six molecules of MeOH in the asymmetric unit. These solvent molecules were refined isotropically, due to their large thermal motions. No hydrogens were added to the solvent molecules, and in the case of several of these molecules their relative populations were assigned values less than one. In addition, the nitrate anion was found to be disordered. The major fragment was refined isotropically with restraints based on bond angles and lengths. Excess electron density around the nitrate group could not be properly modeled. All other non-hydrogen atoms were refined anisotropically. Hydrogen atoms were included but not refined.

The asymmetric unit of **15a** contains the complex cation, a perchlorate anion, four methanol molecules, and one water molecule. The perchlorate is disordered over two sites: $Cl(1)O_4$ is 50% occupied in a general position and $Cl(2)O_4$ is 50% occupied and disordered about a 2-fold axis. The latter was partially resolved [Cl(2) disorder not modeled]. As a result of disorder, the geometry of the perchlorate(s) is not very reliable. The perchlorate oxygen atom O(8) was refined isotropically, while the remaining non-hydrogen atoms were refined anisotropically. Hydrogen atoms associated with the cation and the C−H hydrogens of one MeOH were fixed in calculated positions with O−H = 0.90 Å, N−H = 0.91 Å, and C−H = 0.98 Å; thermal parameters 1.2 times those of the parent atoms; and methyl orientations based on the difference map peak positions where appropriate.

All calculations were performed with the teXsan[30] crystallographic software package and SHELX-97.[27]

Results and Discussion

Characterization of the Complexes. Air-stable crystalline complexes containing the trinuclear $[LnNi_2(trn)_2]^+$ unit were easily produced by adopting the protocol developed for the synthesis of $[LnNi_2(tam)_2]ClO_4$.[21] Unlike the tam system, which only gave trinuclear species when perchlorate salts were employed, the reaction to form $[LnNi_2(trn)_2]^+$ could be carried out with nitrate salts. Nitrate salts were used to produce the complete series of Ln complexes (**1**−**13**).

LSIMS has become the primary diagnostic tool for the detection of cationic *d*/*f* clusters. The spectrum of each complex shows the requisite $[LnNi_2(trn)_2]^+$ parent peak with 100% relative intensity and in good agreement with the calculated isotopic distribution pattern.

As formed in methanolic solution, the complexes have the general formula $[LnNi_2(trn)_2(CH_3OH)]X\cdot mCH_3OH\cdot nH_2O$ (X = ClO_4, NO_3) shown by the X-ray structures of **4a**, **7a**,

(28) Altomare, A.; Burla, M. C.; Cammalli, G.; Cascarano, C.; Guagliardi, A.; Moliterni, A. G. C.; Polidori, G.; Spagna, A. *J. Appl. Crystallogr.* **1999**, *32*, 115.
(29) Buerskens, P. T.; Admiraal, G.; Buerskens, G.; Bosman, W. P.; de Gelder, R.; Israel, R.; Smits, J. M. M. *The DIRDIF94 program system, Technical Report of the Crystallography Laboratory*; University of Nijmegen: Nijmegen, The Netherlands, 1994.
(30) *teXsan: Crystal Structure Analysis Package*; Molecular Structure Corporation, 1995, 1992.

10a, **13a**, and **15a** (vide infra). When the samples are air-dried at room temperature, C, H, N analysis reveals that the crystalline complexes lose both coordinated and free CH_3OH by exchange with ambient H_2O. The dried complexes have the general formula $[LnNi_2(trn)_2(H_2O)]X\cdot nH_2O$ ($X = ClO_4$, NO_3). The replacement of CH_3OH by H_2O is confirmed by the infrared spectra of the complexes, which are very similar for all the dried complexes, with the exception of bands due to the counteranion. For example, IR absorptions for $[ErNi_2(trn)_2(H_2O)]ClO_4\cdot 2H_2O$ (**21**) at 3372 and 540 cm^{-1} indicate the existence of coordinated water; a broad band at 3520 cm^{-1} is due to free water. Bands at 3237 and 3263 cm^{-1} (w, s) result from coordinated NH functions, and ν_3 absorptions associated with ClO_4^- are found at 1088 cm^{-1}. IR absorptions for $[NdNi_2(trn)_2(H_2O)]NO_3\cdot 2H_2O$ (**3**) at 3380 and 540 cm^{-1} indicate the existence of coordinated water; a broad band at 3580 cm^{-1} is due to free water, while bands at 3236 and 3271 cm^{-1}(w, s) result from coordinated NH functions. Bands $\nu_1 + \nu_4$ associated with free nitrate are found at 1762 cm^{-1} (w, s).

X-ray Structures. Since single crystals that appeared to be suitable for X-ray analysis were obtained for most of the complexes, a representative five from across the lanthanide series were chosen for study. These were $[PrNi_2(trn)_2(CH_3OH)]ClO_4\cdot 4CH_3OH\cdot H_2O$ (**15a**), $[SmNi_2(trn)_2(CH_3OH)]NO_3\cdot 4CH_3OH\cdot 2H_2O$ (**4a**), $[TbNi_2(trn)_2(CH_3OH)]NO_3\cdot 4CH_3OH\cdot 3H_2O$ (**7a**), $[ErNi_2(trn)_2(CH_3OH)]NO_3\cdot 6CH_3OH$ (**10a**), and $[LuNi_2(trn)_2(CH_3OH)]NO_3\cdot 4.5CH_3OH\cdot 1.5H_2O$ (**13a**).

The results revealed that the $[LnNi_2(trn)_2]^+$ cations are isostructural in each case. As an example, the structure and atom labeling scheme of the $[LuNi_2(trn)_2]^+$ cation and an expanded view of the coordination spheres of its metallic core are illustrated in Figure 1. Relevant bond length, interatomic distance, and bond angle information for the five cations is given in Table 3. Although the structures were not all measured at the same temperature, the bond lengths obtained are compared directly since the temperature differences and hence the thermal variations are small.

The metallic core of the complex cation $[LnNi_2(trn)_2]^+$ is V-shaped with a value for the angle Ni(1)−Ln(1)−Ni(2) in the range 139.6−143.9°. The Ln^{III} ion is seven-coordinate, being bicapped by two tridentate $[Ni(trn)]^-$ units and coordinated to a single methanol molecule. A detailed analysis[31,32] reveals that the geometry of the Ln^{III} ion is best described as a flattened pentagonal bipyramid. The capping units are nearly identical to each other and in each the Ni^{II} ion is encapsulated by a fully deprotonated $[trn]^{3-}$ ligand via four amine and two phenolato functions, giving an approximately octahedral geometry. The two coordinated phenolato functions bridge to the equatorial plane of the Ln^{III} ion, whereas the free phenolato takes up an axial position. The methanol molecule occupies the remaining equatorial site. Of the bridging phenolato functions, the two (one from each capping unit) that lie trans across Ni^{II} to the apical nitrogen of trn^{3-} (O2 and O4) are coordinated adjacent to each other at the Ln^{III} center, whereas the other two (O1 and O5) are positioned between these and the O-donor of the methanol (O7). For any particular Ln the Ln−O bond distances decrease in the order O7 > O1 > O5 > O4 > O2 > O3 > O6. In the equatorial plane the values are as expected for each Ln^{III} (in the range 2.45−2.54 Å for Pr, 2.41−2.52 Å for Sm, 2.38−2.47 Å for Tb, 2.33−2.43 Å for Er, and 2.33−2.42 Å for Lu). The bonds to the axial phenolates (O3 and O6) are much shorter (from 2.13 Å for Lu−O6 to 2.29 Å for Pr−O3), which is unsurprising because these are the nonbridging donors. Figure 2 reveals that all the Ln−O bond lengths reflect fairly uniformly the periodic decrease in ionic radius of the Ln^{III} ion. The Ni−N and Ni−O bond distances are very similar in all the complexes, falling in the expected range for Ni^{II}, with a mean value of approximately 2.1 Å. Of these, the Ni1−N3 and Ni2−N6 bonds (N3 and N6 are the amine donors associated with the nonbridging phenolates) are the most elongated (2.169−2.235 Å), and the Ni1−O2 and Ni2−O4 bonds (i.e., the Ni−O bonds trans to the apical nitrogen atoms of the ligand) are slightly shortened.

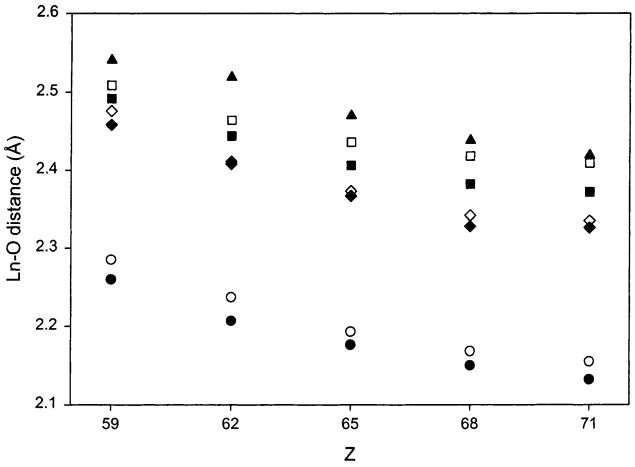

Figure 2. Periodic variation of the various Ln−O bond lengths from the crystal structures of **4a**, **7a**, **10a**, **13a**, and **15a**: (□) Ln−O1; (◆) Ln−O2; (○) Ln−O3; (◇) Ln−O4; (■) Ln−O5; (●) Ln−O6; (▲) Ln−O7.

The fact that in solution the Ni^{II} centers in all the complexes are in comparable coordination environments is demonstrated by their nearly identical visible spectra (see Supporting Information, Figure S1). The absorptions at 960 and 560 nm, using an octahedral model for Ni^{II},[33] can be associated with the $^3A_{2g} \rightarrow {}^3T_{2g}$ and $^3A_{2g} \rightarrow {}^3T_{1g}(F)$ transitions, respectively. An absence of splitting in these bands shows that the two Ni^{II} centers in each individual complex are indistinguishable and therefore suggests that the asymmetry observed between Ni^{II} sites in the solid state is induced by crystal packing.

It is recognized that the coordination number of lanthanide ions tends to decrease with increased atomic number, i.e., as the ionic radius decreases. This is especially prevalent in systems containing coordinated solvent molecules[34] because

(31) Porai-Koshits, M. A.; Aslanov, L. A. *Zh. Strukt. Khim.* **1972**, *13*, 266.
(32) Muetterties, E. L.; Guggenburger, L. J. *J. Am. Chem. Soc.* **1974**, *96*, 1748.
(33) Lever, A. B. P. *Inorganic Electronic Spectroscopy, 2nd ed.*; Elsevier: New York, 1984; p 507.
(34) Martin, L. L.; Jacobsen, R. A. *Inorg. Chem.* **1972**, *11*, 2785.

the lability of the Ln−solvent bond and the lack of geometric preference of the metal ion allows the Ln to select its thermodynamically preferred coordination number. Such a pattern is demonstrated by the previously studied $[LnNi_2(tam)_2]^+$ system.[21] In this series of complexes, from Dy to Yb, the coordination number changes from 7 to 6, respectively, the change occurring through alteration of the number of coordinated solvent molecules. In other cases Ln complexes can contain coordinated anions, e.g., NO_3^- and CH_3COO^-, which compete with solvent or ligand donor atoms for coordination sites. The interplay of these factors, together with the steric preferences of the ligand itself, makes it difficult to predict or control the coordination number or geometry of lanthanide complexes.

The present report provides an extremely rare example of a set of Ln^{III} complexes in which the coordination number and geometry of lanthanide ion do not change at all along the entire Ln series plus lanthanum. Uniquely, they are *d*/*f* complexes and do not contain coordinated counterions. Unfortunately, since the present coaggregated $LnNi_2$ trinuclear complexes are not soluble in water, we have not been able to measure quantitatively their stability constants. However, we did observe that the formation of $[LnNi_2(trn)_2]^+$, unlike the formation of $[LnNi_2(tam)_2]^+$, is insensitive to the nature of the counterion, and this indicates that the $[Ni(trn)]^-$ capping unit is a stronger ligand for Ln^{III} than is $[Ni(tam)]^-$. As a consequence of trn^{3-} being heptadentate, $[Ni(trn)]^-$ possesses a free phenolate donor, whose charge is unmoderated by coordination to the Ni^{II} center. Ln^{III} ions have a well-established preference for hard O^- donors and thus it is likely that the nonbridging phenolate is able to bind strongly to the Ln^{III} center, contributing enough extra stability to the complex to displace NO_3^-. The short Ln−O3 and Ln−O6 contacts observed in the crystal structure corroborate this idea. Because of the short bond distance, the nonbridging phenolates will favor the least crowded coordination sites at the Ln^{III} center, which in this case are the axial sites, leaving the bridging phenolates to fill up the coordination sphere.

It can be presumed that the relative positions of the pair of bridging phenolates in each $[Ni(trn)]^-$ unit are only weakly influenced by the Ln^{III} center and are predetermined by the geometric demands of the trn^{3-} ligand and the Ni^{II} center. The O1−Ni1−O2 and O4−Ni2−O5 angles are thereby restricted, taking values of 77.4−81.3°, which in turn leads to O1−Ln−O2 and O4−Ln−O5 angles of 65.4−67.3° (as determined by the Ln−O distance). The bridging phenolates can therefore fit easily into the pentagonal equatorial plane of the Ln^{III} (where the ideal O−Ln−O angle is 72°), leaving one vacant coordination site for a solvent molecule. On this basis the geometric preference of the system can perhaps be attributed to the mismatch between the geometric requirements of the bridging and nonbridging phenolates. A pentagonal bipyramidal geometry is likely the most efficient way to encapsulate an Ln^{III} ion with a donor set composed of two tightly bound nonbridging phenolates, which prefer to be at the maximum possible angle to adjacent O donors, and two pairs of constrained bridging phenolates, which subtend a relatively small angle at the Ln^{III} center.

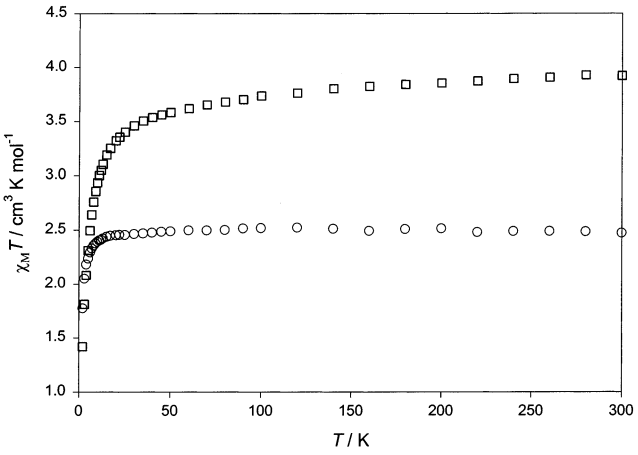

Figure 3. Temperature dependence of χT for (○) **1** and (□) **2**.

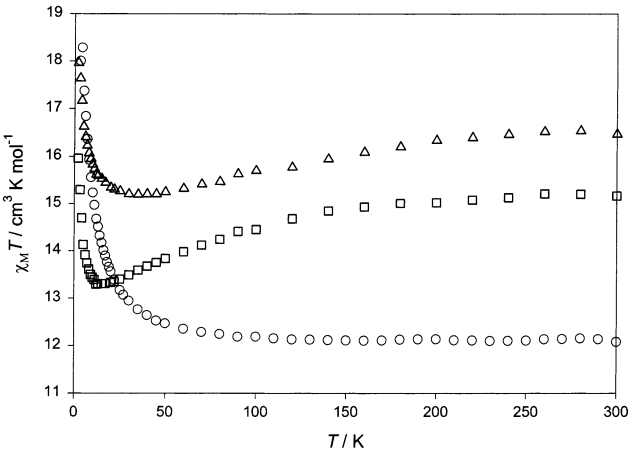

Figure 4. Temperature dependence of χT for (○) **6**, (△) **8**, and (□) **10**.

To reiterate, in contrast to our previous $LnNi_2$ system, not only do the two Ni^{II} centers in a specific complex, and in all the complexes in the present series, have nearly identical distorted octahedral coordination spheres but also the Ln^{III} ions maintain a consistent flattened pentagonal bipyramidal geometry. The $[LnNi_2(trn)_2]^+$ system thus provides an unparalleled opportunity to probe any correlation between the ionic radii of the Ln^{III} ions and the nature of the magnetic exchange interaction between them and the Ni^{II} ions.

Magnetic Properties. Magnetic susceptibilities were measured on powdered samples of **1**−**12** at an applied field of 500 G over the temperature range 2−300 K. Three general patterns of behavior are evident in the χT vs T curves of the complexes containing paramagnetic Ln^{III} ions. The curves for **1**−**5** (illustrated by the curves for **1** and **2**, Figure 3) follow the profile in which χT decreases steadily until, at some point in the low-temperature regime, it starts to decline at an increasing rate and tends to the origin as the temperature approaches zero. The curves for **7**−**10** (illustrated by the curves for **8** and **10**, Figure 4) also show a steady decrease as the temperature is lowered from 300 K but then reach a minimum. Beyond this χT rises sharply, to a maximum at the low-temperature limit. Complex **6** exhibits similar behavior to **7**−**10** at low temperatures (Figure 4). However above ca. 150 K, χT is constant. For **11** and **12** (Figure 5), χT declines steadily with decreasing temperature to below

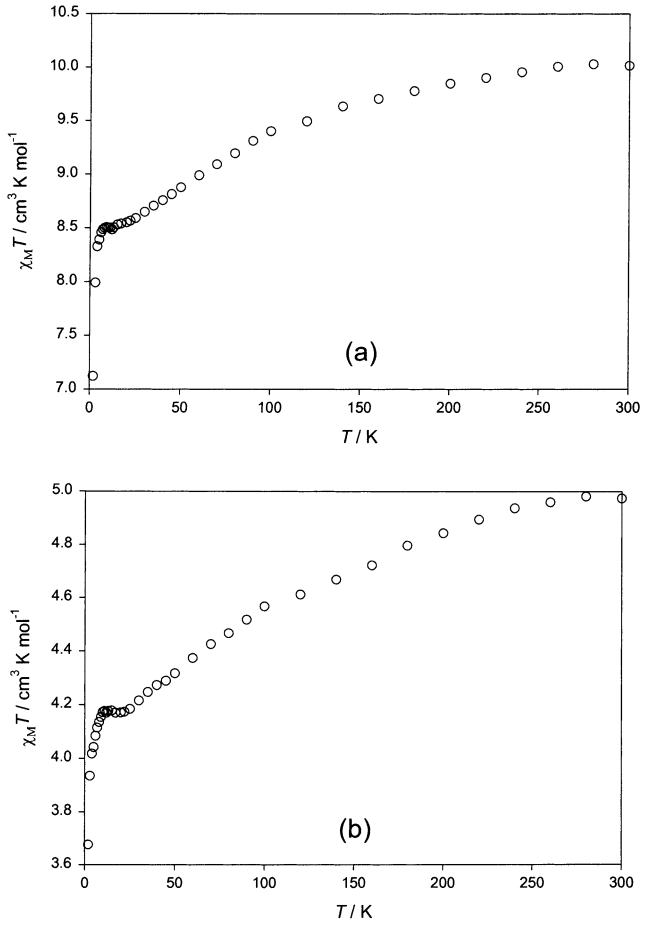

Figure 5. Temperature dependence of χT for (a) **11** and (b) **12**.

Table 4. Magnetic Moment Contributions (μ_B) of the Ln in **2**−**12** at 300 K

complex	Ln	ground state	μ_{eff}	μ_{Ln}	$g[J(J+1)]^{1/2}$
2	Pr	$^3H_4$	5.60	3.40	3.58
3	Nd	$^4I_{4.5}$	5.63	3.44	3.62
4	Sm	$^6H_{2.5}$	4.76	1.69	1.6[a]
5	Eu	$^7F_0$	5.63	3.44	3.61[a]
6	Gd	$^8S_{3.5}$	9.83	8.76	7.94
7	Tb	$^7F_6$	10.83	9.87	9.72
8	Dy	$^6H_{7.5}$	11.48	10.57	10.65
9	Ho	$^5I_8$	11.68	10.80	10.60
10	Er	$^4I_7$	11.01	10.07	9.58
11	Tm	$^3H_6$	8.95	7.76	7.56
12	Yb	$^2F_{3.5}$	6.31	4.47	4.54

[a] $g[J(J+1)]^{1/2}$ does not apply (see text); calculated value is taken from ref 35.

25 K, where there is a point of inflection. The curves then decrease sharply and tend to a minimum at the low-temperature limit. The measured values of μ_{eff} at 300 K for **2**−**12** are listed in Table 4. An initial analysis of the results, described next, shows that, in the high-temperature regime at least, single-ion effects dominate the magnetic properties of these systems.

The central ion in **1** is diamagnetic (La^{III}, f^0, $S = 0$); therefore the magnetization in this sample results only from the two Ni^{II} (d^8, $S = 1$) ions. The Ni^{II} ions are octahedrally coordinated and are expected, therefore, to exhibit spin-only moments modified by the effects of second-order spin−orbit coupling, which leads to a g value in excess of 2.[35] For **1**, μ_{eff} (300 K) = 4.45μ_B, corresponding to two Ni^{II} ions with μ_{eff} (per Ni) = μ_{Ni} = 3.15 and g = 2.23. The χT curve decreases marginally between 300 and 10 K, below which a rather sharp drop due to the effects of zero-field splitting is seen (Figure 3). The magnetic behavior of **1**, as was seen in $[LaNi_2(tam)_2]$,[21] is consistent with the presence of two magnetically isolated octahedral Ni^{II} centers.

By assuming μ_{Ni} = 3.15 (as determined for **1**) and employing

$$\mu_{LnNi_2}{}^2 = \mu_{Ln}{}^2 + 2\mu_{Ni}{}^2 \quad (1)$$

we have calculated the magnetic moments of the various paramagnetic Ln^{III} at 300 K (Table 4). As discussed above, the electronic absorption spectra due to the Ni centers are very similar for all the compounds. This strongly suggests similar Ni(II) crystal fields in all complexes and justifies the use of the same contribution to the overall moment from Ni(II), as an approximation, in all complexes. At room temperature the magnetic moments of the Ln^{III}, except for f^5 and f^6, are expected to approximate those given by[35]

$$\mu_J = g[J(J+1)]^{1/2}\mu_B \quad (2)$$

Except for **4** and **5,** the values obtained are, in fact, in reasonable agreement with the theoretical values derived from eq 2. Complexes **4** (Ln = Sm) and **5** (Ln = Eu) are special cases, because the first excited states of the f^5 and f^6 configurations lie close enough in energy to the ground state to bring first- and second-order Zeeman effects into play. The magnetic moments obtained for these complexes, μ_{Sm} = 1.69μ_B and μ_{Eu} = 3.44μ_B, are within the usually observed ranges (μ_{Sm} = 1.5−1.7μ_B and μ_{Eu} = 3.3−3.5μ_B).

We turn now to a consideration of the possibility of exchange interactions in these systems, which, as indicated by the above analysis, if they are present at all are likely to be relatively weak. The situation with regard to the Gd(III) complex studied here is relatively clear. Because of the $4f^7$ configuration of the Gd(III), the contribution to the overall magnetic moment of **6** from this ion should be spin-only, and in the absence of exchange effects, the moment should be temperature-independent except at low temperatures, where the effects of zero-field splitting of Ni(II) should cause the moment to decrease, as observed for **1** (Figure 3). For the Gd complex, **6**, the observed increase in magnetic moment as the temperature decreases below about 150 K can only be accounted for by the presence of ferromagnetic exchange. This result for **6** is consistent with two other studies that have looked at the Gd^{III}/Ni^{II} couple.[12,13]

In complexes containing Ln ions with configurations other than f^7 (or f^0 or f^{14}) the joint effects of first-order angular momentum and the ligand field lead to anisotropy of the magnetic susceptibility,[8,9,11] and thus the analysis of any exchange interactions becomes a formidable task. On the other hand, qualitative assignment of the magnetic interaction in the absence of data for the isolated Ln^{III} contributions is

(35) Figgis, B. N.; Hitchman, M. A. *Ligand Field Theory and Its Applications*; Wiley-VCH: Toronto, 2000; Chapters 9 and 11.

possible, but only in the case of ferromagnetic exchange. As the various Stark levels of the Ln^{III} become depopulated with decreasing temperature, χT also tends to decrease, such that if χT is observed to *increase* in the complex this indicates a degree of ferromagnetic exchange significant enough to outweigh this depopulation effect. The increase in χT with decreasing T observed at low temperatures for complexes **7**−**10** (shown for **8** and **10** in Figure 4) supports ferromagnetic exchange for the Tb, Dy, Ho, and Er (f^8, f^9, f^{10}, and f^{11}, respectively) systems. The behavior of **7**−**9** corroborates the Ni_3Ln_2 work by Kahn et al.,[13] who observed a ferromagnetic interaction between Tb^{III}, Dy^{III} or Ho^{III}, and Ni^{II}. However, the result for **10** differs from Kahn's findings for Er^{III}, which in the Ni_3Ln_2 system did not display ferromagnetic coupling.

For complexes, **11** and **12** (Figure 5), the observation of a point of inflection in the χT versus T curve near 25 K suggests the possibility of a weak ferromagnetic interaction between Tm^{III} (f^{12}) or Yb^{III} (f^{13}) and the Ni^{II} ions. If this is the situation, then in this case the positive contribution to χT due to the interaction is of such a small magnitude that it only partially offsets the diminishing contribution of the Ln^{III} in a small section of the low-temperature range. Complexes **2**−**5** all exhibit decreasing χT with decreasing T behavior over the entire range of temperatures studied and, for reasons alluded to above, nothing definite can be concluded regarding exchange interactions in these systems.

In light of the above discussion, our published interpretation of the magnetic data from the $[LnNi_2(tam)_2]^+$ system[21] may prove not to be valid. The profile of the μ_{eff} vs T curve for Ln = Dy or Yb, which was assumed to be indicative of an antiferromagnetic interaction because its decline at low T is too steep to be due solely the zero-field splitting of the Ni^{II} ions, could simply be accounted for by the diminishing contribution of the Ln^{III} ion. In addition, saturation effects due to the magnitude of the magnetic field (10 000 G) used in those earlier experiments[21] may have masked the presence of any magnetic interactions.

Conclusions

By use of a simple one-pot synthesis, the amine phenol ligand H_3trn allows the preparation (from methanolic solution) of complexes whose cations have the formula $[LnNi_2(trn)_2(CH_3OH)]^+$. Remarkably, irrespective of the Ln, the cations are isostructural, the Ln^{III} being coordinated in a flattened pentagonal bipyramidal geometry by the O donors of two nearly identical $[Ni(trn)]^-$ units and a methanol molecule. Trn^{3-} is heptadentate and, as a result, having bound Ni^{II} in an octahedral N_4O_2 environment, retains a free phenolate donor. The negative charge on this phenolate, unlike that on the bridging phenolates, is unmoderated by contact with Ni^{II} and thus gives rise to stronger Ln−O bonding. The stability of the system is such that $[Ni(trn)]^-$ can displace nitrate from $Ln(NO_3)_3$, where $[Ni(tam)]^-$, which possesses only bridging phenolates, cannot. The mismatch between the spatial requirements of these donors and the bridging phenolates, which are constrained by coordination to the Ni^{II}, may account for the uniform adoption of pentagonal bipyramidal geometry by all the Ln^{III}. The reported series of isostructural complexes is ideal for a study of the *d*/*f* magnetic interaction between Ni^{II} and the various Ln^{III}.

Currently there is no theoretical model available that can reliably account for the orbital angular momentum effects of both the Ln^{III} and the Ni^{II}, and thus a quantitative analysis of our variable-temperature magnetic susceptibility data was not possible. (We are hopeful that the increasing supply of data on *d*/*f* complexes from this study and others will spur the development of such a model.) At the qualitative level, results from complexes **6**−**12** indicate that a ferromagnetic interaction occurs between Gd^{III}, Tb^{III}, Dy^{III}, Ho^{III}, Er^{III} (and possibly Tm^{III} and Yb^{III}) and Ni^{II}. In fact, this study is in very good agreement with a theoretical model from Kahn in which he predicted that Ln^{III} with f^7−f^{13} configurations would give ferromagnetic coupling.[36]

Acknowledgment is made to the Natural Sciences and Engineering Research Council of Canada for the provision of operating grants (R.C.T. and C.O.) and to the Royal Society, U.K., for a postdoctoral fellowship (S.R.B.).

Supporting Information Available: UV−Vis spectra of **4**, **8**, **13** and **14** and CIF files for **4a**, **7a**, **10a**, **13a**, and **15a**. This material is available free of charge via the Internet at http://pubs.acs.org.

IC0205278

(36) Andruh, M.; Ramade, I.; Codjovi, E.; Guillou, O.; Kahn, O.; Trombe, J. C. *J. Am. Chem. Soc.* **1993**, *115*, 1822.